Laser magnetic resonance study of the gas phase reactions of OH with CO, NO, and NO_2

Carleton J. Howard

Aeronomy Laboratory, NOAA Environmental Research Laboratories, Boulder, Colorado 80302

K. M. Evenson

National Bureau of Standards, Boulder, Colorado 80302

(Received 18 April 1974)

COPY

A laser magnetic resonance spectrometer has been used in combination with a discharge-flow system to measure the gas phase reaction rates of the OH radical with CO, NO, and NO_2 at 296 °K and over a pressure range 0.4–5 torr. For the bimolecular reaction $OH + CO \rightarrow CO_2 + H$ we measure a rate constant, $k = 1.56 \times 10^{-13}$ cm^3/molecule · sec. For the termolecular reactions $OH + NO + M \rightarrow HNO_2 + M$, $M = He$, $k = 4.0 \times 10^{-31}$ cm^6/molecule^2 · sec; $M = Ar$, $k = 4.4 \times 10^{-31}$ cm^6/molecule^2 · sec; $M = N_2$, $k = 7.8 \times 10^{-31}$ cm^6/molecule^2 · sec. For the reaction $OH + NO_2 + N_2 \rightarrow HNO_3 + N_2$, $k = 2.9 \times 10^{-30}$ cm^6/molecule^2 · sec. Laser magnetic resonance detection of radicals is shown to be extremely sensitive, linear, and versatile. A complete description of this technique is presented with a discussion of its potential in the study of the reactions of free radicals.

I. INTRODUCTION

Laser magnetic resonance (LMR) was first developed to study the rotational Zeeman spectra of O_2.[1] The original spectrometer used a 337 μm HCN laser and had the absorption cell outside the laser cavity. Since then, the sensitivity of the system has been increased considerably by locating the absorption cell inside the laser cavity[2] and by using an improved infrared detector. Spectra of the stable paramagnetic molecules NO and NO_2 have been studied,[3,4] and recently the transient free radicals OH, CH, HO_2, and HCO have also been observed.[5–8]

The LMR technique offers very high sensitivity, 2×10^8 OH molecules/cm^3, for example, compared with sensitivities of approximately 2×10^{12} molecules/cm^3 with ESR, about 10^{11} molecules/cm^3 with uv ($A\ ^2\Sigma^+ \leftarrow X\ ^2\Pi$) resonance absorption, and about 3×10^9 molecules/cm^3 with uv resonance fluorescence using a water vapor discharge light source. The highest sensitivity for OH, about 3×10^6 molecules/cm^3, has been obtained with resonance fluorescence using a frequency doubled dye laser light source. The combination of high sensitivity and versatility makes the LMR method particularly attractive in the study of the reaction chemistry of triatomic radicals such as HO_2 which are generally studied by indirect methods in which the radical is not detected.

In order to test the usefulness of the LMR system for kinetic measurements we have selected several important and interesting reactions of OH for the first investigation. The reaction with CO,

$$OH + CO \rightarrow CO_2 + H\ , \tag{1}$$

is probably the most frequently studied OH reaction and provides a convenient standard since its rate constant is moderately large and not strongly temperature dependent. This reaction is an important step in most combustion and atmospheric mechanisms.[9]

The reactions of OH with NO and NO_2,

$$OH + NO + M \rightarrow HNO_2 + M \tag{2}$$

and

$$OH + NO_2 + M \rightarrow HNO_3 + M\ , \tag{3}$$

represent radical chain terminating reactions. These reactions are particularly important to the development of accurate models describing the chemistry of normal and polluted atmospheres.[10–12] Most of the active chemical processes in the atmosphere below 50 km altitude involve one or more radical reactants, and Reactions (2) and (3) are important as major sinks for three reactive atmospheric molecules.

These results are discussed and compared with other measurements.

II. EXPERIMENTAL

A. Apparatus

The general technique of laser magnetic resonance is very similar to other magnetic resonance methods such as ESR and NMR. While NMR uses radio frequency radiation to produce transitions between nuclear spin levels, and ESR uses microwave radiation to produce transitions between electron spin levels, LMR uses radiation in the far infrared to produce transitions between rotational levels in paramagnetic molecules. Absorption is accomplished by tuning the molecule into resonance with a far infrared laser by means of a magnetic field.

A simplified rotational energy level diagram illustrating the mechanism of laser magnetic resonance absorption is shown in Fig. 1. The energy is not given to scale in order to illustrate the effect of magnetic splitting of the rotational levels, and not all the levels which arise from Λ doubling and nuclear spin are shown. The near coincidence of the laser line E_L with the field free rotational transition $E(J = \frac{5}{2} \leftarrow J = \frac{3}{2})$ is shown on the left. The symbols + and − under the rotational quantum number J indicate the parity of the Λ doublet components

 Copyright © 1974 American Institute of Physics

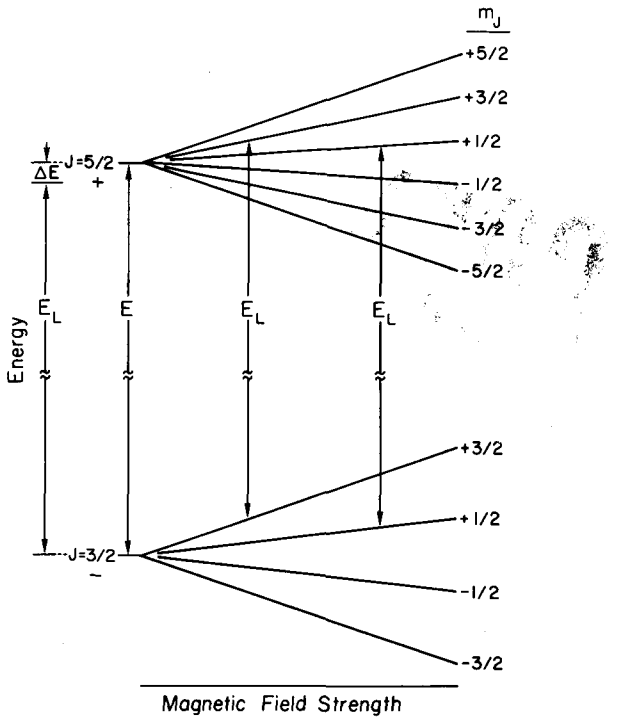

FIG. 1. Rotational energy level diagram showing near coincidence of laser line E_L with rotational transition $E(J=\frac{5}{2} \leftarrow J=\frac{3}{2})$ on the left and the magnetic field splitting of the rotational states producing resonant absorption between sublevels at two magnetic field strengths. Note that the energy scale has been greatly compressed to illustrate the effect of the magnetic splitting to make up the field free energy difference ΔE.

shown. ΔE, the difference between E and E_L, is usually of the order of less than 1% of E and can be either positive or negative. When a magnetic field is applied, each rotational level is split into $2J+1$ sublevels. In this example, absorption occurs at two values of magnetic field strength, when allowed transitions ($\Delta M_J = 0$) between the magnetic sublevels are resonant with the laser radiation.

The strongest absorptions are due to electric dipole transitions. The appropriate selection rules are determined by the polarization of the laser radiation relative to the magnetic field, with $\Delta M_J = 0$ for parallel polarization ($E_\omega \parallel H$) and $\Delta M_J = \pm 1$ for perpendicular polarization ($E_\omega \perp H$). The selection rules for the weaker magnetic dipole transitions are $\Delta M_J = \pm 1$, ($E_\omega \parallel H$) and $\Delta M_J = 0$ ($E_\omega \perp H$). More detailed discussions of the spectroscopic applications of LMR are given in references cited earlier.[3-8]

The attenuation of the laser radiation by absorption is generally a small fraction of the output power, therefore it is necessary to modulate the magnetic field and use phase sensitive detection of the laser signal. A schematic diagram of the apparatus is shown in Fig. 2. The laser oscillates in a resonant cavity defined by two gold coated spherical mirrors with radii of approximately 11 and 7 m. One mirror is attached to a micrometer drive, which is used to adjust the length of the cavity to the peak of the laser line. The wavelength of the lasing line is identified by measuring the distance between successive cavity resonances. Continuous wave lasing is produced by a dc discharge (5–8 kV at 0.3–0.8 A) in a 68 mm i.d. by 4 m long tube containing a low pressure (0.6–0.8 Torr, 1 Torr = 133.3 Pa) H_2O/H_2 or D_2O/D_2 gas mixture.[13] Laser wavelengths of 78.4, 79.1, or 118.6 μm with H_2O/H_2 mixtures and 84.3 or 107.7 μm with D_2O/D_2 mixtures are commonly used. Most of the operating wavelengths have been determined by very accurate frequency measurements, allowing identification of the energy levels in the water molecule which give rise to lasing.[13]

The laser cavity is divided into two sections by a 3×10^{-3} cm thick polyethylene film window. The window serves three purposes: (1) It provides a vacuum seal between the laser discharge and the absorption region; (2) it acts as a partial reflector to couple a small fraction of the laser radiation out of the cavity to a detector, and for this purpose, the angle of the window with respect to the axis of the laser is adjustable near the Brewster angle; and (3) it restricts the laser radiation to a single linear polarization, which can be oriented either parallel ($E_\omega \parallel H$) or perpendicular ($E_\omega \perp H$) to the magnetic field in the absorption region. This feature is important in spectroscopic applications of the LMR system, because it is often possible to identify transitions by the different selection rules that operate for each polarization.

The laser operates on a single frequency and has a very narrow bandwidth. Single frequency operation is possible because the mode spacing (about 40 MHz) is much wider than the laser gain curve (about 6 MHz). An iris is used to eliminate off axis modes. A measurement of the frequency stability of a similar laser at 78.4 μm[14] showed a drift of less than 1 MHz for a period of about $\frac{1}{2}$ h.

Two types of detectors are used. A Golay cell is used to make test measurements and adjustments on the laser, and a liquid helium cooled germanium bolometer

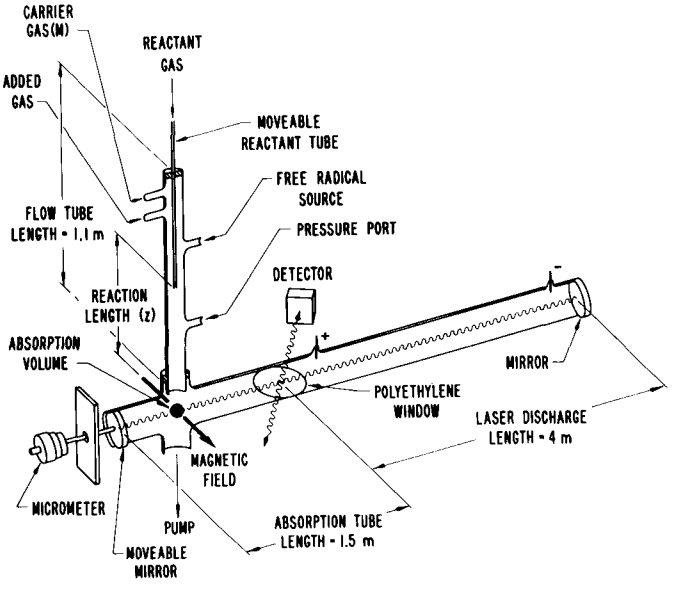

FIG. 2. Schematic diagram of laser magnetic resonance system with flow reactor used in kinetic studies.

is used for radical detection. The bolometer offers several advantages over other detectors, since it is very sensitive (noise equivalent power is 1×10^{-12} W/Hz$^{1/2}$ at 320 Hz) and has a relatively high frequency response (about 75% of dc at 1 kHz). Normal total power output levels from the laser are from 1–100 μW. The power absorbed by radicals is between 0.3 and about 10^{-4} of the total laser power.

A uniform magnetic field (indicated as an arrow in Fig. 2) is produced by a 38.1 cm electromagnet with 14 cm ring shimmed pole tips and a 5.08 cm air gap. Fields up to 23.5 kG can be obtained in the absorption volume. An adjustable field modulation of up to 100 G at 270 Hz is used to obtain the modulated absorption signal. The absorption volume is a small region, about 2 cm^3, defined by the intersection of the mutually perpendicular laser beam, homogeneous magnetic field, and the flow tube axis.

The flow tube is vertical as shown in Fig. 2. Two different 1.1 m long flow tubes made from precision bore Pyrex tubing, 1.905 and 2.54 cm i.d., were used. The carrier gas, helium, argon, or nitrogen, which is normally more than 98% of the total gas flow, enters the flow tube at the top, flows down the tube, passes through the intersection with the laser absorption tube, and is evacuated by the action of a 10 liter/sec mechanical pump. Average flow velocities range between 100 and 1200 cm/sec. OH radicals are produced in the carrier stream by the fast reaction of NO_2 with H atoms,

$$H + NO_2 \rightarrow OH + NO \ . \qquad (4)$$

The NO_2 is added through the added gas port about 7 cm downstream from the carrier gas inlet and H atoms are generated in a 2450 MHz microwave discharge in a side tube and are added through a third port labeled "free radical source" in Fig. 2. Generally the NO_2 is added slight excess to assure rapid conversion of the H to OH. The excess NO_2 does not interfere with the other reaction processes. In the OH + CO reaction study, however, excess NO_2 would cause a problem since the H atoms generated by reaction with CO would reform OH. Therefore, all measurements on this reaction were made under the condition of excess H and very small NO_2 flows.

The inside surface of the flow tube has been coated with phosphoric acid or boric acid to inhibit the destruction of radicals on the Pyrex wall. The phosphoric acid coating was prepared by boiling the standard laboratory reagent (86% H_3PO_4) to produce a heavy syrup which was applied while warm with a glass wool brush. The boric acid coating was prepared by dissolving about 30 g of H_3BO_3 per liter of water and was applied by rinsing the flow tube. Although both coatings were about equally effective in reducing radical wall loss, boric acid was preferred because it is less corrosive and easier to apply and remove.

The reactant gas, CO, NO, or NO_2, is injected by means of a moveable stainless steel tube into the carrier stream containing the OH radicals. The reactant tube is 1.2 m long by 3.18 mm o.d. and is attached to a scale which is used to measure its position over the range of z(10–50 cm) from the absorption volume. The moveable injector is preferred over the variable reacant flow method of deriving rate data for two reasons: (1) There is no danger of altering the lineshape of the absorption curve by pressure or collision broadening, since only the reaction time is changed and not the reactant gas pressure and (2) the absolute value of the reaction length z does not have to be accurately measured, since relative values are adequate. The latter is an important consideration because the flow tube is terminated in a larger cross section absorption tube, making it difficult to accurately determine the transit time of the reaction gas mixture from the end of the flow tube to the absorption volume.

Thermal conductivity mass flowmeters are used to measure flow rates. The flowmeters were calibrated using three different techniques. For large flow rates (200–20 STP cm^3/sec, STP ≡ 0 °C, 760 Torr) a wet test meter was used; for medium flow rates (50–0.05 STP cm^3/sec) the pressure drop across a viscous flow element was used; and for small flow rates ($0.5\text{–}10^{-3}$ STP cm^3/sec) the pressure rate of change in a calibrated volume was used. The agreement of these overlapping methods was excellent, within 2%, and the error in all flow measurements is less than 5%.

The low vapor pressure and the dimerization of NO_2 made it necessary to measure all NO_2 flows by the rate of pressure change in a calibrated volume.

A capacitance manometer was used to measure the flow tube pressure. The factory calibration of the pressure meter was checked using a water manometer, and pressure measurements were accurate to within 2%.

Most gases were taken directly from high pressure cylinders with no special purification or trapping. The manufacturer stated minimum purity levels are as follows: He > 99.999% (analyzed); Ar > 99.999%; N_2 > 99.999%; H_2 > 99.95%; CO > 99.99% (analyzed).

The NO was purified by passing the gas from a cylinder through a refrigerated (– 77 °C) Pyrex coil containing silica gel. This procedure is very effective for removing most of the other oxides of nitrogen,[15] and therefore the reactive impurities in NO. The NO_2 impurity, for example, should be much less than 0.1% after trapping.

NO_2 was purified by successive vacuum distillations of the cylinder gas at – 196, – 77, and 0 °C and stored as a liquid in a stainless steel cylinder. The color of the purified solid and vapor pressure of the liquid indicated that other nitrogen oxides and low boiling gases were adequately removed.

B. Technique and analysis

Although it was known that the laser magnetic resonance technique was very sensitive for detecting free radicals, it had not been previously established that the measured absorption signal was proportional to the radical number density. As with other magnetic resonance methods using modulated absorption, the absorption signal is detected as the derivative of the absorption curve. Because the linewidth may depend upon radical concen-

tration, there is a possibility that one or more integrations of the derivative curve would be necessary to obtain a measurement of relative radical concentrations.

A typical absorption trace taken with a pen recorder is shown in Fig. 3. Several tests were made to demonstrate that the peak to peak amplitude, indicated by the symbol a in Fig. 3, is proportional to the number density of absorbing radicals in the absorption volume. First, several derivative absorption lines recorded at different radical concentrations were integrated to see if the lineshape changed with radical concentration. When no variation was detectable, a second test was made by measuring the derivative amplitude a as a function of radical concentration. The measurements are shown in Fig. 4. NO_2 was used as an absorbing molecule because it is chemically stable in the flow system and therefore its absolute concentration is easily measured. The data are plotted on a logarithmic scale to display the two decade range of linearity. The measurements were made by adding small flows of NO_2 (9×10^{-4}–9.3×10^{-2} STP cm^3/sec) to a large flow of helium (4.89 STP cm^3/sec) in order to maintain a constant total pressure which was independent of NO_2 addition rates in the flow tube. This procedure eliminates problems resulting from line shape changes due to pressure broadening.

An additional test was made to determine if the rate constant data were dependent upon the transition which was used to monitor the OH concentrations. No variation was observed when measurements using an ($X^2\Pi_{3/2}$, $v=0$, $J=\frac{5}{2}\leftarrow J=\frac{3}{2}$) transition at 118.6 μm were compared with ($X^2\Pi_{3/2}$, $v=0$, $J=\frac{7}{2}\leftarrow J=\frac{5}{2}$) measurements at 84 μm. This result is reasonable when one considers that the OH rotational levels are in equilibrium and that relaxation occurs at nearly gas kinetic collision rates.[16]

Thus, we have concluded that measurements of relative radical concentrations are easily obtained from LMR spectrometer data by measuring the peak to peak amplitude of the derivative curves. Care is always taken to assure that there are no changes in the experimental parameters which affect line shape, i.e., gas pressure, modulation amplitude, and detector time constant, during the period in which a single set of relative concentration measurements are made.

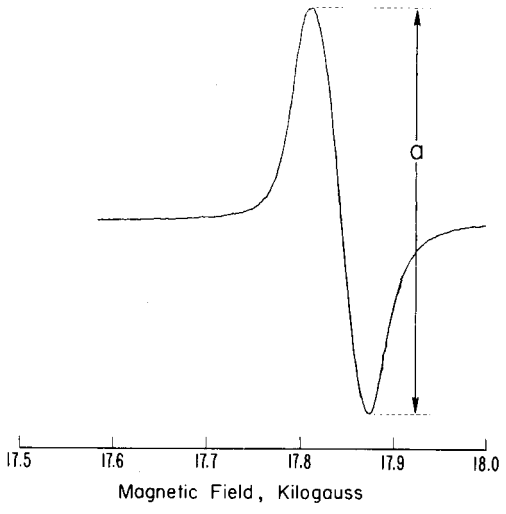

FIG. 3. Pen recording of OH derivative absorption line observed using the 84 μm D_2O laser with the radiation electric field polarized parallel to the magnetic field ($E_\omega \| H$). The peak to peak amplitude a is proportional to the number of OH radicals. The hyperfine splitting due to the hydrogen nucleus is not observable because of the large modulation broadening of the line.

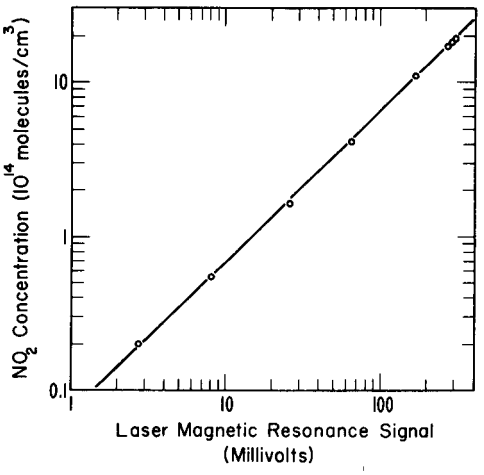

FIG. 4. Plot of NO_2 number density vs LMR signal, demonstrating that the amplitude of the derivative curve is directly proportional to the number of radicals in the absorption volume. The 84 μm D_2O laser was used ($E_\omega \| H$) for making measurements with the first line of the NO_2 triplet at 7.39 kG. The total pressure was about 3.1 Torr and the helium carrier gas flow was about 4.89 STP cm^3/sec.

We have also observed that the fluctuations in the sensitivity of the detection system are negligible (less than 3%) for periods of about 15 min, the time required for taking data for a single rate constant determination. The LMR signal is surprisingly insensitive to laser power. For example it changes less than 10% when the laser power is reduced by a factor of four by changing the discharge current.

The high sensitivity of LMR offers the advantage of studying reactions as pseudo-first-order radical loss processes, where relative radical concentration measurements are adequate. In general, the methods and analysis used here are identical to those described by others[17,18] employing flow systems. The remainder of this section will describe the methods and tests which were made to demonstrate the reliability of the analysis in our application.

It is assumed that the bulk properties of the gas stream, temperature, pressure, and flow velocity are determined by the carrier gas flow. The concentrations of carrier gas, reactant gas, and OH molecules are in the ranges $(20–1)\times10^{16}$, $(50–1)\times10^{13}$, and $(300–1)\times10^{9}$ molecules/cm^3, respectively.

Figure 5 is a plot of the axial OH concentration profile in the flow tube. The OH radicals are generated by Reaction (4) from hydrogen atoms produced in a microwave discharge in a mixture of helium and hydrogen. The gas flow through the discharge is normally very small (about

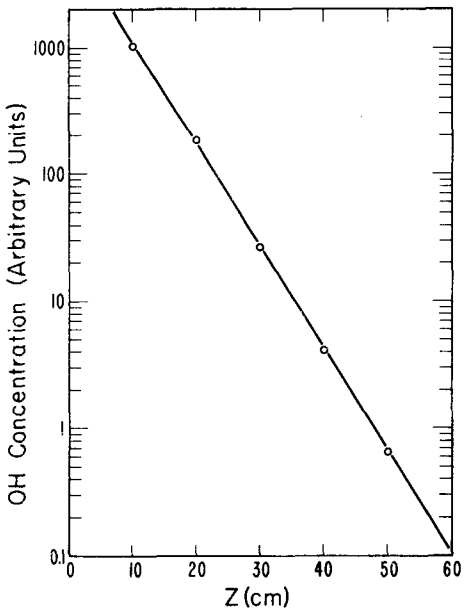

FIG. 5. OH radical axial profile produced by wall loss mechanism in 2.54 cm diameter flow tube with boric acid coating. Helium carrier gas flow rate = 1.85 STP cm^3/sec, total pressure = 2.54 Torr, $k_w = 38$ sec^{-1}, and $\gamma = 1.6 \times 10^{-3}$. The reaction length z is the distance between the end of the moveable reactant tube and the absorption volume.

0.05 STP cm^3/sec of He and < 0.01 STP cm^3/sec of H_2) and is not a significant perturbation on the carrier gas flow. To take the data in Fig. 5, a moveable OH source was obtained by adding a small flow of NO_2 to the carrier gas stream through the moveable reactant tube. Thus it was possible to directly measure the OH loss processes occurring in the absence of all other reactants. From the linearity of the semilog plot it is evident that the OH loss rate is purely first order and may be described by the rate equation

$$d(\mathrm{OH})/dt = k'(\mathrm{OH}) \ , \tag{5}$$

where k' is the first order decay rate constant. This may be rewritten in the integrated form

$$(\mathrm{OH})_z = (\mathrm{OH})_0 \exp(-k'z/\bar{v}) \ , \tag{6}$$

where the flow system substitution $t = z/\bar{v}$ has been made, z is the distance from the end of the moveable inlet to the absorption volume (as shown in Fig. 2), and $\bar{v}$ is the average flow velocity of the gas stream.

If one makes the reasonable assumption that the only effect of moving the point of addition of NO_2 is to vary the location of the OH source, i.e., that the precursor, H atom, concentration does not change significantly down the tube, $k' = k_w$, the first order wall loss constant. The value of γ, the fraction of OH–wall collisions which destroy the OH, is readily calculated from the value of k_w,[17]

$$\gamma = 2rk_w/\bar{\omega} \ , \tag{7}$$

where r is the tube radius and $\bar{\omega}$ is the average molecular velocity for OH. For OH radicals, values of γ are $(1-2)\times 10^{-3}$, similar to the observations of Anderson and Kaufman[19] and Westenberg and de Haas.[20] Since a typical value of γ for H atoms[21] is between $10^{-6} - 10^{-5}$, the heterogeneous loss of H is negligible compared to OH, as assumed.

This measurement of the wall loss rate also allows an estimate of the sensitivity of the system to be made. The estimate is based on experiments in which a small measured NO_2 flow was added to a carrier gas stream containing excess H atoms. It was assumed that one OH radical was generated for each NO_2 molecule added. The OH concentration in the absorption region was calculated using the measured OH wall loss rate. The corresponding LMR signal was compared to the noise level with a 1 sec time constant to derive a sensitivity of about 2×10^8 OH/cm^3 for a signal to noise ratio of 1.

The absence of any second order OH loss eliminates the necessity of considering radical–radical reactions such as

$$\mathrm{OH} + \mathrm{OH} \rightarrow \mathrm{H_2O} + \mathrm{O} \tag{8}$$

and

$$\mathrm{O} + \mathrm{OH} \rightarrow \mathrm{O_2} + \mathrm{H} \tag{9}$$

in analyzing rate data. These reactions often make a significant contribution to the over-all OH loss rate in systems used to study OH reactions and may contribute serious errors to attempts to derive rate data.[9] A further estimate of the importance of other secondary reactions can be made based upon the OH concentrations ($< 3\times 10^{11}$ molecules/cm^3) in the flow tube. Even if one assumes a very large rate constant of 10^{-11} cm^3/molecule · sec, the first order rate constant for loss of OH due to secondary reactions is less than 3 sec^{-1}, which is small compared to 20–90 sec^{-1} for the reaction rates. Also, since we observed no variations in the measured rate constants at different initial OH concentrations, we conclude that secondary reactions are negligible.

The axial pressure gradient dp/dz (Torr/cm) may be estimated for Poiseuille flow by

$$dp/dz = 6.0\times 10^{-3}\eta\bar{v}/r^2 \ , \tag{10}$$

where η is the carrier gas viscosity in poise. The largest relative error $\Delta p/p$ occurs at the lowest pressure and highest flow velocity. For a 50 cm reaction zone, $\Delta p/p \cong 7\%$ in the worst case. The errors contributed by this effect are reduced by measuring the average flow tube pressure near the middle of the reaction zone and no further corrections are applied.

Since the average flow velocity $\bar{v}$ of the carrier gas is taken as the average transport velocity for OH radicals in the measurement of the rate constants, it is assumed (1) that the radicals are uniformly distributed across the diameter of the flow tube, i.e., no radial concentration gradients, and (2) that the transport of radicals along the axial concentration gradient produced by reaction is negligible. Kaufman[17] has discussed the errors contributed to flow reactor rate measurements by these effects.

First, because there is a very significant destruction rate of OH on the wall, it is clear that there must be some radial concentration gradients. However, if ra-

dial diffusion is sufficiently rapid the concentration will be nearly uniform and the effect can be ignored. Estimates of the magnitude of radial concentration gradients can be made using the equation derived by Kaufman[17] and diffusion coefficients estimated from the data compiled by Marrero and Mason.[22] For the range of first order wall and homogeneous reaction rates encountered here, diffusion is estimated to be sufficiently rapid in helium at pressures less than about 5 Torr. The reliability of this estimate has been demonstrated by studying the pressure dependence of the purely bimolecular reaction of OH with CO up to 30 Torr. The measured rate constant did not change up to about 8 Torr then fell off about 20% in the range up to 30 Torr. A similar but more pronounced effect was found in argon and nitrogen, for nitrogen the onset was near 3 Torr and the falloff was about 60% at 30 Torr. This difference is probably due to the low diffusion coefficients of OH in argon and nitrogen gases. Since the pressure dependence of the termolecular reactions of NO and NO_2 with OH is an important measurement, an attempt was made to extend the pressure range by employing an empirical correction based on the OH–CO measurements to data on these reactions. This was unsuccessful, however, because of a very large scatter in the high pressure data. The scatter may have resulted from the high sensitivity of the radial gradient effect to the wall loss rates,[17] which are not perfectly reproducible in the different reactions.

Some difficulty in the high pressure rate constant measurements was also caused by poor mixing of the reactant gas with the carrier stream at high flow velocities ($\bar{v} \cong 1000$ cm/sec). The problem was alleviated by injecting the reactant gas through a small perforated loop of Teflon tubing attached to the end of the moveable reactant tube.

There have been other observations of difficulities in attempts to measure OH rate constants in flow reactors at high pressures. Anderson *et al.*[23] have attributed the pressure dependence of the NO_2 reaction[19] to improper radial mixing. Poirier and Carr[24] have made an analysis of the OH radial concentration profiles produced by concurrent first and second order reactions superimposed on Poiseuille flow. However, we feel that the uncertainties involved in making corrections to the high pressure data are too large to warrant the effort, and only low pressure results are reported.

The effects of axial diffusion are more readily dealt with. A first order correction can be estimated from the relationship[17]

$$k_c = k'(1 + k'D/\bar{v}^2) , \qquad (11)$$

where k_c is the corrected first order reaction rate constant, k' is the measured first order rate constant, and D is the OH–carrier gas binary diffusion coefficient in cm^2/sec. The correction is largest at low pressures, where it is estimated to be about 6% in helium at 0.5 Torr (the worst case). The helium carrier gas data were adjusted accordingly, as discussed later, but since the diffusion coefficients for OH in argon and nitrogen are about one-third the value for helium, the correction is neglected for these gases.

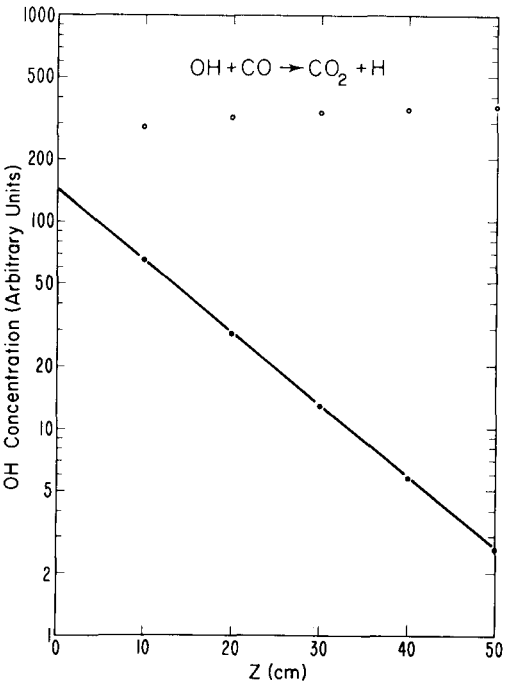

FIG. 6. Semilog plot of OH signal vs reaction length z for the reaction of CO with OH in 2.54 cm diam tube. Total flow rate = 5.20 STP cm^3/sec, CO flow rate = 0.0712 STP cm^3/sec, and the flow tube pressure = 1.009 Torr. The open circles are points taken by moving the reactant tube with no CO flow. The closed circles show OH falloff due to reaction and include a correction for the loss of OH on the reactant tube.

A small correction is also made for the destruction of OH on the surface of the moveable reactant tube. This effect is very reproducible and is observed as a small increase in the OH signal as the injector is withdrawn from the gas stream. The change results from the reduction of the area of the reactant tube exposed to the OH stream. This effect is shown in Fig. 6 by the open circles, which are the OH signal with no CO reactant added through the moveable tube. Each reaction data point (closed circles) has been corrected downward by the factor that the injector increases the signal in the blank run. Note that the correction is quite small compared to the change produced by reaction.

Bimolecular rate constants are calculated from first order decay plots, such as Fig. 6, by dividing the first order rate constant, k' (sec^{-1}) as in Eq. (6), by the reactant number density (molecules/cm^3). Termolecular rate constants are the slope of a graph of the effective bimolecular rate constants as a function of the buffer gas (M) number density and will be discussed later.

The accuracy of the measurements based upon a consideration of systematic errors in the flow rate, pressure, and reaction length measurements is about 8%. This can be compared with a standard deviation of about 5% for the CO reaction. However, because of other less tangible uncertainties, such as the validity of the bulk flow model used in the analysis, we consider a factor of ±15% as a reasonable estimate of the accuracy of the rate constants with 90% confidence.

TABLE I. Summary of OH + CO → reaction measurements (296 °K).

Rate constant (k_1) (10^{-13} cm^3/molecule · sec)	OH detection method	Rate measurement technique	Reference
1.56 ± 0.2	Laser magnetic resonance	Discharge flow	This work
1.45 ± 0.22	uv resonance absorption	Flash photolysis	Smith and Zellner[28]
1.62 ± 0.08	uv resonance fluorescence	Flash photolysis	Davis[29]
1.33	Electron spin resonance	Discharge flow	Westenberg and de Haas[20]
1.35 ± 0.2	uv resonance fluorescence	Flash photolysis	Stuhl and Niki[30]
1.42	Kinetic spectroscopy	Flash photolysis	Greiner[31]
1.91 ± 0.08	Electron spin resonance	Discharge flow	Dixon-Lewis *et al.*[27]
1.66 ± 0.5	Mass spectrometer[a]	Discharge flow	Mulcahy and Smith[25]
1.73 ± 0.02	Mass spectrometer[a]	Discharge flow	Wilson and O'Donovan[26]

[a]OH was not detected. Rate constant determined from mass spectrometer analysis of other species.

III. RESULTS AND DISCUSSION

A. $OH + CO \xrightarrow{k_1} CO_2 + H$ [Reaction (1)]

The CO reaction rate constant reported is an average of 21 measurements in helium (8), argon (10), and nitrogen (3). The correction for axial diffusion discussed earlier [Eq. (11)] was applied to the measurements in helium, using a diffusion coefficient of 500 Torr · cm^2/sec. This correction raised the average for all the measurements only 1% but reduced the standard deviation by about 10%.

A summary of measurements from the literature of the OH–CO rate constant k_1 at room temperature is presented in Table I for comparison with the present measurement. The error limits are those of the (sometimes highly optimistic) authors. The general agreement is quite good, especially considering the widely different techniques employed. Four different OH detection schemes and two different rate methods were used. The two mass spectrometer measurements[25,26] are set apart because OH was not detected.

Westenberg and de Haas[20] recently point out that the earlier work in their laboratory, Dixon-Lewis *et al.*,[27] is probably an overestimation of the rate constant because the following was neglected: (1) OH wall loss and (2) the second order OH reaction, Reaction (8). Corrections for axial diffusion and wall loss are included in the Westenberg and de Haas measurement.[20]

Smith and Zellner,[28] Davis,[29] and Stuhl and Niki[30] employed static photolysis systems. OH radicals were generated by flash photolysis of H_2O or by photolytic $O(^1D)$ formation followed by the rapid reaction with H_2 or H_2O. The OH decay was monitored by OH ($A\,^2\Sigma - X\,^2\Pi$) resonance fluorescence[29,30] or resonance absorption.[28] The dimensions of the reaction vessels were large and the operating pressures were high so as to make wall loss negligible. Also, the relative OH/CO concentrations are adjusted to minimize the second order OH reaction. The greatest uncertainties in these measurements are probably due to the rather small range of OH decay and problems of preparing and then maintaining quantitative mixtures of buffer, OH source, and reactant gases in the reaction cell. However, the method is extremely versatile for variable temperature and high pressure reaction rate studies.

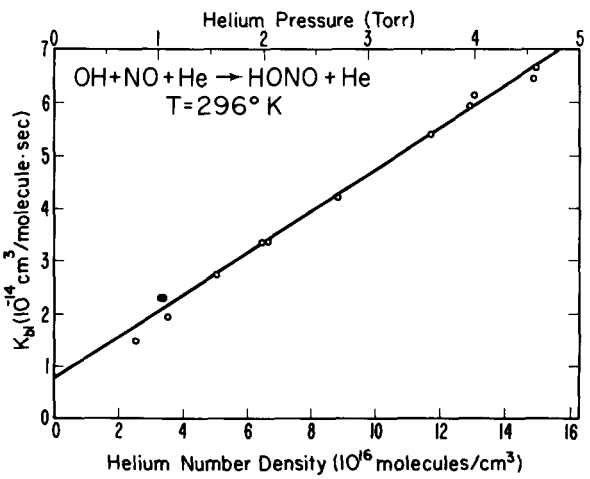

FIG. 7. Plot of effective bimolecular rate constants k_{bi} for NO reaction measured with 1.905 cm diam flow tube. Slope $= k_2$ (M = He) = 3.98 (σ = 0.10) × 10^{-31} cm^6/molecule^2 · sec; σ = standard deviation of the slope.

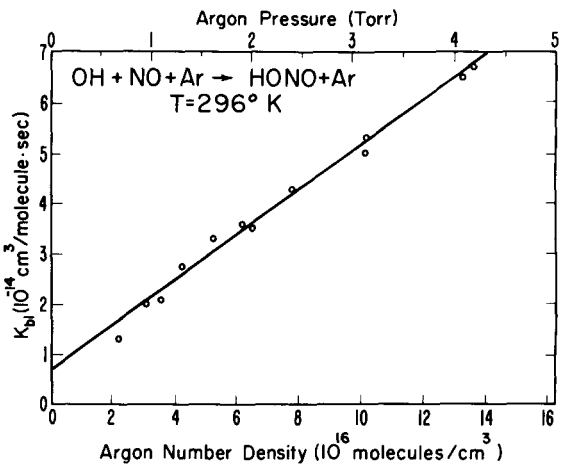

FIG. 8. Plot of effective bimolecular rate constants k_{bi} for NO reaction measured with 2.54 cm diam flow tube. Slope = k_2 (M = Ar) = 4.45 (σ = 0.13) × 10^{-31} cm^6/molecule^2 · sec; σ = standard deviation of the slope.

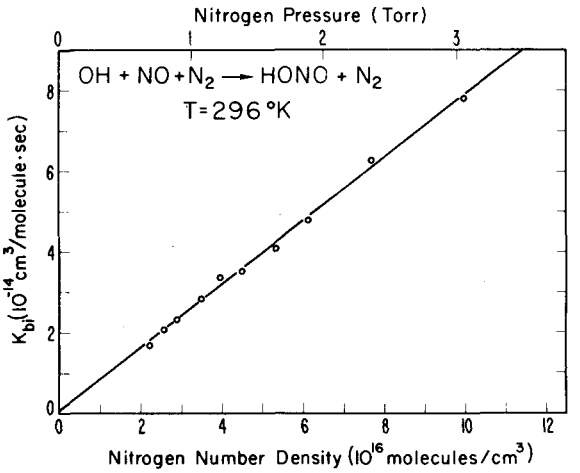

FIG. 9. Plot of effective bimolecular rate constants k_{bi} for NO reaction measured with 2.54 cm diam flow tube. Slope $= k_2$ ($M = N_2$) $= 7.85\ (\sigma = 0.17) \times 10^{-31}$ cm^6/molecule^2 · sec; σ = standard deviation of the slope.

The rate constant reported for Greiner[31] is the average of four measurements made at 300–305 °K, three of which were reanalyzed from earlier work.[32] His method was to flash photolyze H_2O_2 and to measure OH decay rates using kinetic spectroscopy.

Mulcahy and Smith[25] and Wilson and O'Donovan[26] have reported values of the OH + CO rate constant from discharge-flow mass spectrometer measurements. The methods are similar to the earlier work of Herron[33] and are based on an analysis of the CO_2 product in reaction mixtures of H added to excess NO_2 and CO.

Wilson and O'Donovan[26] have redone the measurement of Herron and attribute the discrepancy in his low result to (1) improper correction for Reaction (8), (2) neglect of wall loss, and (3) neglect of any reaction of OH with excess NO_2. They independently derive $k_1 = 1.5 \times 10^{-13}$ cm^3/molecule · sec but adjust this value up about 15% based on their measurement of k_1/k_8 and the rate for Reaction (8) from Dixon-Lewis *et al.*[27]

In their study, Mulcahy and Smith[25] extended the mass spectrometer analysis to the detection of H_2, H_2O, NO, O_2, and NO_2 in addition to CO_2. They also investigate the kinetics of the H/NO_2/CO system under conditions of excess H. They conclude that there are significant wall loss processes. In excess NO_2, if all OH losses not accountable by reactions with OH, O, and CO are attributed to a single $OH + NO_2 \rightarrow HNO_3$ mechanism, an estimate of the NO_2 reaction rate can be made, following the analysis of Wilson and O'Donovan.[26] This estimate will be discussed later.

The first six measurements in Table I are probably the most reliable. The average of these, $k_1 = 1.46 \times 10^{-13}$ cm^3/molecule · sec, would seem to be the best estimate for the rate constant, and all six values are within 10% of this value.

B. $OH + NO + M \xrightarrow{k_2} HNO_2 + M$

Rate constants for the termolecular reactions of OH are the slope of a plot of the effective bimolecular rate constant k_{bi} versus buffer gas (M) number density, for a series of measurements at different pressures. The data for the NO reactions are shown in Figs. 7–9 for M = He, Ar, and N_2. The solid straight lines are least-squares fits to the equally weighted data. The standard deviations of the slopes were about 3% of the slope. Only termolecular kinetics are observed at the relatively low pressures covered in this study. A summary of these and other measurements is presented in Table II.

If the gas phase termolecular reaction were the only OH loss process for the NO reaction, the data in Figs. 7–9 should extrapolate to a $k_{bi} = 0$ intercept at zero pressure. The nonzero intercept is taken as evidence of a heterogeneous (OH + NO + wall) process as observed in the work of Anderson *et al.*[23] and Westenberg and de Haas.[34,35] However, it should be noted that this wall reaction does not affect the results and that the termolecular rate constant does not depend upon the wall condition. Although the magnitude of the intercept does de-

TABLE II. Summary of OH + NO + M → reaction measurements (296 °K).

Rate constant (k_2) (10^{-31} cm^6/molecule^2 · sec)	OH detection method	Rate measurement technique	References
		M = He	
4.0 ± 0.6	Laser magnetic resonance	Discharge flow	This work
3.3 ± 0.7	uv resonance fluorescence	Discharge flow	Anderson *et al.*[23]
4.1 ± 0.6	uv resonance absorption	Flash photolysis	Morley and Smith[39]
8	Electron spin resonance	Discharge flow	Westenberg and de Haas[34]
8	uv resonance fluorescence	Flash photolysis	Stuhl and Niki[a]
		M = Ar	
4.4 ± 0.7	Laser magnetic resonance	Discharge flow	This work
3.4 ± 0.7	uv resonance fluorescence	Discharge flow	Anderson *et al.*[23]
3.6	Electron spin resonance	Discharge flow	Westenberg and de Haas[34]
4.0 ± 2	uv resonance fluorescence	Discharge flow	Anderson and Kaufman[19]
		$M = N_2$	
7.8 ± 1.2	Laser magnetic resonance	Discharge flow	This work
5.8 ± 1.2	uv resonance fluorescence	Discharge flow	Anderson *et al.*[23]

[a]F. Stuhl and H. Niki, J. Chem. Phys. 57, 3677 (1972).

TABLE III. Summary of $OH + NO_2 + M \rightarrow$ reaction measurements (296 °K).

Rate constant (k_3) (10^{-30} cm^6/molecule · sec)	OH detection method	Rate measurement technique	Reference
	$M = N_2$		
2.9 ± 0.44	Laser magnetic resonance	Discharge flow	This work
2.3 ± 0.5	uv resonance fluorescence	Discharge flow	Anderson *et al.*[23]
2.0 ± 0.5	uv resonance fluorescence	Discharge flow	Anderson and Kaufman[19]
	$M = He$		
1.0 ± 0.2	uv resonance fluorescence	Discharge flow	Anderson *et al.*[23]
1.1	uv resonance absorption	Flash photolysis	Morley and Smith[39]
1.6	Electron spin resonance	Discharge flow	Westenberg and de Haas[34]
~2	Competitive reaction[a]	Photolysis	Simonaitis and Heicklen[36]
<17	Mass spectrometer[a]	Discharge flow	Mulcahy and Smith[25]
	$M = Ar$		
1.0 ± 0.2	uv resonance fluorescence	Discharge flow	Anderson *et al.*[23]
1.0 ± 0.3	uv resonance fluorescence	Discharge flow	Anderson and Kaufman[19]
0.8	Electron spin resonance	Discharge flow	Westenberg and de Haas[34]
	$M = Kr$		
0.0036	Competitive reaction[a]	Photolysis	Bérces and Förgeteg[37]
	$M = H_2O$		
15	Competitive reaction[a]	Photolysis	Simonaitis and Heicklen[36]

[a]OH not detected, see text.

pend upon the wall condition and flow tube diameter, the termolecular rate constant (slope) does not.

In Table II, there are three values of k_2 (M = He) near 4×10^{-31} cm^6/molecule^2 · sec and two near 8×10^{-31}. It is not clear what the origin of the discrepancies might be. All of the measurements of Anderson *et al.*[23] are about 20% lower than ours. Although this difference is within the error limits of the measurements, it suggests a systematic error in one or both sets of measurements.

C. $OH + NO_2 + M \xrightarrow{k_3} HNO_3 + M$ [Reaction (3)]

The reaction of OH with NO_2 was studied only in nitrogen buffer gas, as shown in Fig. 10. Our measurement and the results of others are summarized in Table III. All values are for the termolecular low pressure rate constant k_3.

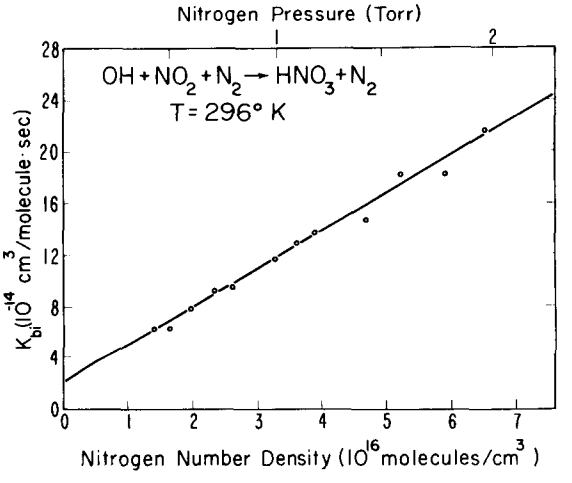

FIG. 10. Plot of effective bimolecular rate constants k_{bi} for NO_2 reaction measured with 2.54 cm diam flow tube. Slope $= k_3 (M = N_2) = 2.93$ ($\sigma = 0.1$) $\times 10^{-30}$ cm^6/molecule^2 · sec; σ = standard deviation of the slope.

Two of the measurements, Simonaitis and Heicklen[36] and Bérces and Förgeteg,[37] use indirect methods. In these measurements, the rate constant determination is based upon (1) the relative yields of stable products formed in irradiated gas mixtures, (2) an assumed reaction mechanism, and (3) comparison with a known reaction rate constant. Simonaitis and Heicklen, for example, measure CO_2 yields from photolyzed mixtures of NO_2, H_2O, and CO. Their estimate of k_3 is based upon the rate constant for the OH + CO reaction. Their values in Table III assume $k_1 = 1.5 \times 10^{-13}$ cm^3/molecule · sec. Some of the discrepancy in their measurement of the temperature dependence of Reaction (3) is removed if one assumes the very recent determinations[20,28,29] of the activation energy of Reaction (1) in lieu of the recommendation of the review of Baulch *et al.*[38]

Bérces and Förgeteg[39] estimate k_3 from a measurement of its rate relative to the reaction

$$OH + HNO_3 \rightarrow H_2O + NO_3 \qquad (12)$$

in photolyzed mixtures of NO_2 and HNO_3. Morley and Smith[39] give a critique of their assumed mechanism in order to account for the factor of 2000 disagreement.

The method of Mulcahy and Smith[25] was discussed earlier. The value given for k_3 is actually the total rate constant for three mechanisms: (1) first order OH wall loss, (2) the heterogeneous reaction ($OH + NO_2 +$ wall) and (3) the termolecular Reaction (3). Their measurement, therefore, is likely to be too high.

In general, there are larger discrepancies between the recent measurements of the reaction of OH with NO and NO_2 than between the measurements of the reaction

with CO. However, most of the direct measurements agree well with the present results. Therefore, we feel that rate constants near our values are the most reliable estimates.

We now hope to extend the application of the laser magnetic resonance spectrometer–flow reactor combination to the study of the rates and mechanisms of the free radicals such as HCO and HO_2, whose chemistry have remained uncertain for lack of a sufficiently sensitive detector.

ACKNOWLEDGMENTS

This work has been supported in part by the NBS Measures for Air Quality Program. We also express our appreciation to Dr. A. L. Schmeltekopf, who first suggest the usefulness of LMR for kinetic measurements.

[1]K. M. Evenson, H. P. Broida, J. S. Wells, R. J. Mahler, and M. Mizushima, Phys. Rev. Lett. **21**, 1038 (1968).
[2]J. S. Wells and K. M. Evenson, Rev. Sci. Instrum. **41**, 226 (1970).
[3]M. Mizushima, K. M. Evenson, and J. S. Wells, Phys. Rev. A **5**, 2276 (1972).
[4]R. F. Curl, Jr., K. M. Evenson, and J. S. Wells, J. Chem. Phys. **56**, 5143 (1972).
[5]K. M. Evenson, J. S. Wells, and H. E. Radford, Phys. Rev. Lett. **25**, 199 (1970).
[6]K. M. Evenson, H. E. Radford, and M. M. Moran, Jr., Appl. Phys. Lett. **18**, 428 (1971).
[7]H. E. Radford, K. M. Evenson, and C. J. Howard, J. Chem. Phys. **60**, 3178 (1974).
[8]C. J. Howard and K. M. Evenson (unpublished work).
[9]W. E. Wilson, Jr., J. Phys. Chem. Ref. Data **1**, 535 (1972).
[10]G. Brasseur and M. Nicolet, Planet. Space Sci. **21**, 939 (1973).
[11]H. Levy, II, Planet. Space Sci. **21**, 575 (1973).
[12]P. J. Crutzen, Ambio **1**, 41 (1972).
[13]W. S. Benedict, M. A. Pollack, and W. J. Tomlinson III, IEEE J. Quantum Electron **QE5**, 108 (1969).
[14]K. M. Evenson, J. S. Wells, L. M. Matarrese, and L. B. Elwell, Appl. Phys. Lett. **16**, 159 (1970).
[15]E. E. Hughes, J. Chem. Phys. **35**, 1531 (1961).
[16]B. Stevens, *The International Encyclopedia of Physical Chemistry and Chemical Physics, Topic* 19. *Gas Kinetics, Vol.* 3, *Collisional Activation in Gases* (Pergamon, Oxford, England, 1967), p. 130.
[17]F. Kaufman, *Progress In Reaction Kinetics* (Pergamon, New York, 1961), Vol. 1, p. 1.
[18]H. Niki, E. E. Daby, and B. Weinstock, *Twelfth Symposium (International) on Combustion* (The Combusion Institute, Pittsburgh, PA, 1969), p. 277.
[19]J. G. Anderson and F. Kaufman, Chem. Phys. Lett. **16**, 375 (1972).
[20]A. A. Westenberg and N. de Haas, J. Chem. Phys. **58**, 4061 (1973).
[21]D. O. Ham, D. W. Trainor, and F. Kaufman, J. Chem. Phys. **53**, 4395 (1970).
[22]T. R. Marrero and E. A. Mason, J. Phys. Chem. Ref. Data **1**, 3 (1972).
[23]J. G. Anderson, J. J. Margitan, and F. Kaufman, J. Chem. Phys. **60**, 3310 (1974).
[24]R. V. Poirier and R. W. Carr, Jr., J. Phys. Chem. **75**, 1593 (1971).
[25]M. F. R. Mulcahy and R. H. Smith, J. Chem. Phys. **54**, 5215 (1971).
[26]W. E. Wilson and J. T. O'Donovan, J. Chem. Phys. **47**, 5455 (1967).
[27]G. Dixon-Lewis, W. E. Wilson, and A. A. Westenberg, J. Chem. Phys. **44**, 2877 (1966).
[28]I. W. M. Smith and R. Zellner, J. C. S. Faraday II, **69**, 1617 (1973).
[29]D. D. Davis, AIAA Paper No. 73-501, AIAA/AMS International Conference on the Environmental Impact of Aerospace Operations in the High Atmosphere, Denver, CO, June 11–13, 1973.
[30]F. Stuhl and H. Niki, J. Chem. Phys. **57**, 3671 (1972).
[31]N. R. Greiner, J. Chem. Phys. **51**, 5049 (1969).
[32]N. R. Greiner, J. Chem. Phys. **46**, 2795 (1967).
[33]J. T. Herron, J. Chem. Phys. **45**, 1854 (1966).
[34]A. A. Westenberg and N. de Haas, J. Chem. Phys. **57**, 5375 (1972).
[35]A. A. Westenberg and N. de Haas, J. Phys. Chem. **76**, 1586 (1971).
[36]R. Simonaitis and J. Heicklen, Int. J. Chem. Kinetics **4**, 529 (1972).
[37]T. Bérces and S. Förgeteg, Trans. Faraday Soc. **66**, 640 (1970).
[38]D. L. Baulch, D. D. Drysdale, and A. C. Lloyd, "High Temperature Reaction Rate Data," No. 1, Dept. of Physical Chemistry, Leeds University, England, 1968).
[39]C. Morley and I. W. M. Smith, J. Chem. Soc. Faraday II **68**, 1016 (1972).